Elsevier Editorial System(tm) for Journal of Food Engineering

Manuscript Draft

Manuscript Number: JFOODENG-D-17-01095R1

Title: Effects of Ball Milling on the Structural, Thermal, and Rheological Properties of Oat Bran Protein Flour

Article Type: SI:FSD 2016

Keywords: oat protein; FTIR spectroscopy; DSC; amylose-lipid complex; dispersion.

Corresponding Author: Mr. Kurnia Ramadhan, M.Sc

Corresponding Author's Institution: University of Nottingham

First Author: Kurnia Ramadhan, M.Sc

Order of Authors: Kurnia Ramadhan, M.Sc; Tim J Foster, PhD

Abstract: Oat bran protein flour (OBPF), containing protein, starch, and lipid as major constituents, was ball milled and subsequently evaluated on structural conformation, thermal properties, particle size distributions, and rheological properties. Prior to ball milling, characterisation of OBPF were conducted by means of Fourier transform infrared (FTIR) spectroscopy and differential scanning calorimetry (DSC) showing the existence of aggregated protein and starch-lipid complexes as predominant constituents of OBPF. Ball milling altered structural conformations of both protein and starch. Moreover, increase of ball milling time gradually decreased the transition enthalpy changes of amylose-lipid complexes upon heating which can be related to disruption of amylose-lipid complexes helical structure. Ball milling at higher speed resulted to smaller average particle size distributions of OBPF. Dynamic mechanical spectra of concentrated dispersions containing ball milled OBPF exhibited lower storage (G') and loss (G") moduli compared to control sample due to reduced particles volume packing. Moduli-frequency sweep data satisfactory fitted the Power Law's model.

22nd of October 2017

Journal of Food Engineering

Resubmission of manuscript JFOODENG-D-17-01095R1

Dear Editor,

Thank you for the opportunity to revise our manuscript. We appreciate the careful review and constructive suggestions. The manuscript has been rewritten base on the suggestions, with a new title "Effects of Ball Milling on the Structural, Thermal, and Rheological Properties of Oat Bran Protein Flour". Following this letter are our responses to the reviewers' comments, including how and where the text was modified.

Thank you for your considerations.

Most sincerely,

Kurnia Ramadhan

Detailed Response to Reviewers

Reviewer #1

Comments	Responses
The manuscript reports a study on structural issues of an oats bran protein concentrate using spectroscopy, calorimetry and rheology. Standard procedures were used, but for a publication in Journal of Food Engineering, I was expecting a better quantitative analysis than presented. For example, the rheograms (moduli-frequency) could be modelled to obtain parameters than can be statistically compared. The manuscript is weak in statistics, even though the effects of milling and fractionation or defatting of the concentrate are discussed. A properly revised manuscript would meet the quality required for the journal.	The manuscript has been rewritten and added with more quantitative data presented in tables.
Lines 223-225: Consider including the statistics (+- standard deviation, SD or standard error of mean, SEM) of the particle sizes.	Revised as suggested. These lines have been rewritten and can be found in revised manuscript starting from the Line 255.
Lines 243-252: It would have been better to model the moduli-frequency relationships to obtain quantitative parameters for a deeper	Revised as suggested. These lines have been rewritten and can be found in revised manuscript starting from the Line 284.

analysis of the results, trends and effects of milling. A sentence like "However, the slope of G' and G" versus frequency curves seems to remain unchanged … of OBPC dispersion", is too qualitative and eye-balling for the journal.	
Figure 3: Is it not possible to define some quantitative parameters from the spectra to characterize the samples? I was thinking absorbance units at those specified wavenumbers for protein structures could be used. Absorbance units at certain wavenumbers are used in FTIR studies on starches to properly characterize amorphous and crystalline structures in them.	Revised as suggested.
Figure 7: Consider modelling the rheograms for quantifiable characterization parameters to deeply discuss the rheological behaviours of the samples.	Frequency sweep data have been fitted to the Power Law's model and presented in table. The rheogram remain unchanged.
Table 1: Better to include the statistics to justify using 'significant', 'significantly different' or 'not significant' in the text (lines 205, 233 and 247, for example). This table could also contain the characterization parameters for the rheological behaviours of	The words "significantly" have been removed. Fitting parameters of frequency sweep tests have been added.

the samples.	

Reviewer #2

Comments	Responses
Line 15: Instead of "Fourier Transform Infrared", "Fourier transform infrared" is more appropriate.	Revised as suggested. This line has been rewritten and can be found in revised manuscript starting from the Line 14.
Lines 25-26, 44-45, 58-63, 82-83, 185-187, 192-193, 206-207, 215-216: These sentences should be revised.	Revised as suggested. These lines have been rewritten.
In the manuscript, 35 references were used. From these references, only 9 references were published within the last 8 years (since 2010). This means that the authors have not mentioned from recent studies sufficiently.	References have been updated.
Lines 30-46: "Introduction" section should be re-written. Literature studies given in this section is not sufficient.	Revised as suggested. These lines have been rewritten and can be found in revised manuscript starting from the Line 27.
Line 63: Please use small letters in the spelling of "Propanol".	Revised as suggested. This line has been rewritten and can be found in revised manuscript starting from the Line 65.
Line 111: The abbreviation of second is not "sec".	Revised as suggested. This line has been rewritten and can be found in revised manuscript starting from the Line 128.

Line 138: Please use subscript for "2" in "-CH2-".	Revised as suggested. This line has been rewritten and can be found in revised manuscript starting from the Line 158
Lines 254-259: Important numerical results should be indicated in "Conclusions" section.	Revised as suggested. These lines have been rewritten and can be found in revised manuscript starting from the Line 296.

Reviewer #3

Comments	Responses
This manuscript deals with the influence of chemical features and ball milling on the structuring characteristics of oat bran protein. For this purpose, several experimental tests were performed. The research topic falls within the scope of the Journal of Food Engineering and could be of the scientific interest. Nevertheless, the content of the manuscript evidence some lacks that must be improved. Please consider the following comments:	The manuscript has been rewritten and added with more quantitative data presented in tables.
Keywords: Personal consideration: Words included in the title should be removed from keywords section.	Revised as suggested.
Introduction: This section should be extended to include updated references in	Revised as suggested.

the field (last 5 years).	
Materials and methods: Replicates should be included in all sections.	Revised as suggested.
Further detail why experimental conditions were selected or some reference should be included in some methods section (see as e.g. ball milling procedure, preparation of OBPC dispersions, among others).	Revised as suggested.
Figure 6. Log representation is commonly used for rheological measurements.	Revised as suggested.
References should be updated: Only 3 references from last 5 years.	References have been updated.
Tbale 1. Standard deviations should be included.	Revised as suggested.

Highlights

- Ball milling alters structural conformations of aggregated proteins and starch-lipid complexes
- Mechanical impact caused by ball milling disrupted the ordered structure of amylose-lipid complexes
- Changes in mechanical moduli of dispersions are mainly contributed by differences in particle size distributions after ball milling

Effects of Ball Milling on the Structural, Thermal, and Rheological Properties of Oat Bran Protein Flour

Kurnia Ramadhan [a,b,*] and Tim J. Foster [a]

[a] *Division of Food Sciences, University of Nottingham, Sutton Bonington Campus, Leicestershire LE12 5RD, United Kingdom*

[b] *Department of Food Technology, Universitas Bakrie, Jakarta 12920, Indonesia*

*Corresponding Author:

Email address: kurnia.ramadhan@nottingham.ac.uk (Kurnia Ramadhan)

Abstract

Oat bran protein flour (OBPF), containing protein, starch, and lipid as major constituents, was ball milled and subsequently evaluated on structural conformation, thermal properties, particle size distributions, and rheological properties. Prior to ball milling, characterisation of OBPF were conducted by means of Fourier transform infrared (FTIR) spectroscopy and differential scanning calorimetry (DSC) showing the existence of aggregated protein and starch-lipid complexes as predominant constituents of OBPF. Ball milling altered structural conformations of both protein and starch. Moreover, increase of ball milling time gradually decreased the transition enthalpy changes of amylose-lipid complexes upon heating which can be related to disruption of amylose-lipid complexes helical structure. Ball milling at higher speed resulted to smaller average particle size distributions of OBPF. Dynamic mechanical spectra of concentrated dispersions containing ball milled OBPF exhibited lower storage (G') and loss (G") moduli compared to control sample due to reduced particles volume packing. Moduli-frequency sweep data satisfactory fitted the Power Law's model.

Keywords: oat protein, FTIR spectroscopy, DSC, amylose-lipid complex, dispersion.

1. Introduction

Interests in protein-rich foods are rising favoured by its health-promoting effects. The benefits of dietary protein intake has been associated with body weight management and maintenance of muscle mass and function (Deutz et al., 2014; Westerterp-Plantenga et al., 2017). The urge to search for alternative food protein sources have led to valorisation of underexploited plants and side stream agricultural products.

Oat bran is a by-product of oat flour milling and have been used as a fibre-enriching ingredient. Although oat bran contains abundance of protein, its full utilisation remains challenging. Enzymatic pre-treatment of oat bran thick cell walls is necessary to assist protein extraction, otherwise a highly alkaline pH is required to release protein that adversely affect the nutritional quality (Jodayree et al., 2012). Low solubility of oat protein in slightly acidic to neutral pH range also restrict its applicability for foods (Konak et al., 2014). In order to bridge the gap between the limitations and advantages of oat bran protein for utilisation in foods, a feasible separation technique has been introduced to obtain protein-enriched flour with low degree of purity (Sozer et al., 2017). The presence of protein, starch and lipid, as constituents of composite flour, are known contributing to the physicochemical properties and functionality of flour (Puncha-Arnon and Uttapap, 2013; Saleh, 2017).

Physical modification of food materials by means of ball milling has gained attention due to ability in changing functionality. The modified functionality can be attributed to alteration in structural conformation as found in ball milled starch and starch-enriched food materials (Dhital et al., 2011; Liu et al., 2011; Roa et al., 2014a). However, there are limited studies reporting the effects of ball milling on structural conformation changes in food proteins including whey and soy protein (Liu et al., 2017; Sun et al., 2015).

This present study aims to evaluate the alteration on structural conformation of chemical constituents within ball milled oat bran protein flour, and subsequently to extrapolate the conformational changes into the thermal and rheological properties of its dispersion. This study would provide useful insights to extend the utilisation of oat bran protein flour in food formulations.

2. Materials and methods

2.1. Materials

Oat bran protein flour (OBPF) was supplied by Tate & Lyle Oat Ingredients (Kimstad, Sweden) as a brand of PrOatein®. This material was in the form of coarse powder and declared to have ca. 94% dry matter containing 54% protein, 17% fat, 18% carbohydrate, and 2% fibre on a dry basis. This material was prepared from oat bran that have gone through enzymatic, thermal, and physical separation processes.

2.2. Elimination of lipid and starch

Elimination of lipid and reduction of starch were intended to provide a correct assignment of FTIR spectra bands and interpretation of thermal properties in the later analyses. Lipid were extracted using solvent in soxhlet apparatus as described by Pandey and Shrivastava (Pandey and Shrivastava, 2017) with modifications. Two solvents with different polarity were used, i.e. hexane for the non-polar solvent, and isopropanol for the polar solvent. Defatted samples are addressed as NPDO for the hexane-defatted OBPF and PDO for the isopropanol-defatted OBPF. Protein extraction from defatted samples, i.e. NPDO and PDO, did not lead to reasonable protein yields for further analysis. Therefore, in this study, starch reduction was chosen to obtain a higher protein concentration. Starch reduction was conducted by dispersing and stirring the defatted

samples into alkaline solution for 30 min as described by De Souza et al. (De Souza et al., 2016). The sample was then lyophilised to obtain dry powder and addressed as APDO.

2.3. Ball milling procedure

Ball milling was carried out by using Planetary Micro Mill (Pulverisette 7 classic line, FritschGmbH, Germany) as described by Abbaszadeh et. al. (2014) with modifications. Two and a half grams of OBPF was put into 12 ml grinding bowl containing 6 Zirconium dioxide grinding balls. High speed milling was run at 800 revolutions per minute (rpm) for 15 min. The low speed milling was carried out at 200 rpm for 240 min. The applied milling cycle configuration was 5 min milling followed by 5 min rest to dissipate heat. Reversed milling directions were set to prevent ball slippage at both milling speeds.

2.4. Preparation of OBPF dispersions

OBPF dispersions (5%, 20%, and 30% wt) were prepared by suspending the flour into distilled water as described by Roa et al. (Roa et al., 2015) with modifications. These concentrations were selected according to previous trials conducted with OBPF dispersions from 5% to 30% wt. A dilute system (5% wt) was selected to evaluate the particle size distributions, while the 20% wt dispersion was subjected to thermal analysis for its flow-ability reason, and the 30% wt dispersion was selected for rheological analysis to avoid sedimentation.

2.5. Attenuated total reflectance – Fourier transform infrared (ATR-FTIR) spectroscopy

The infrared spectra were obtained by using a Bruker Tensor 27 System (Bruker Optik GmbH, Ettlingen, Germany) equipped with diamond Attenuated Total Reflection (ATR) crystal and operated using OPUS software version 7.2.139.1294. The tests were

performed at ambient temperature. The open-air background test was run prior to sample measurement. Approximately 50 mg of dry sample was placed into contact with the diamond ATR crystal and sample holder. Each absorbance measurement was conducted under 128 scans with 4 cm^{-1} resolutions. The presented infrared spectra were obtained as a mean from three measurements of duplicate samples that have undergone normalisation and baseline correction. Height of peaks were determined by calculating the absorption intensity differences between peak and its own baseline. Peak height ratio of selected absorption bands was used to quantify the infrared spectral changes. The amide I band, i.e. ~1630 cm^{-1}, was selected as reference band in evaluating spectral changes due to elimination of lipids and starch. Calculation of absorbance intensity ratio ~997 to ~1022 cm^{-1} was used to assess structural conformation changes on starch as described by Liu et al. (Liu et al., 2011). The use of second derivative spectra was intended to resolve the overlapping bands both in amide and saccharide regions (Figure 3). The assignment of protein secondary structure within amide I band referred to a study reported by Tang and Ma (2009). Further processing of infrared spectra was conducted using Spectragryph optical spectroscopy software version 1.0.2 (https://www.effemm2.de/spectragryph/).

2.6. Micro-differential scanning calorimetry

Scanning calorimetry was performed in a Micro-Differential Scanning Calorimeter III (Setaram Instrumentation, France). About 800 mg of dispersions containing 20%wt solid sample was transferred into hermetically sealed sample vial made from hastelloy, while similar weight of deionized water was used as reference. Heating-cooling processes were performed in two cycles from 20 to 120 ^{o}C at a rate of 1 $^{o}C\ min^{-1}$. Measurement was run in duplicate for each sample. The heat flow curves were processed using Calisto Processing

software v1.43 (AKTS, Switzerland) to obtain the maximum heat absorption temperatures (T_m) and the transition enthalpy changes (ΔH).

2.7. Particle size distributions

Particle size and size distributions were measured based on the principles of light scattering using LS13320 Laser Diffraction Particle Size Analyzer (Beckman Coulter, High Wycombe, UK). A dispersion of 5% OBPF in distilled water was pipetted into a liquid module sample cell. The measurement was run for 60 s under following conditions: Fraunhofer theory was used as optical model treating particles in spherical approximation, refractive indexes of dispersant and sample were 1.33 and 1.6 respectively. The particle size was determined by the volume-weighted mean diameter size. Each measurement was run in duplicate.

2.8. Rheology

Structuring properties of OBPF dispersion was evaluated using rheological analysis. Small deformation tests of oat dispersion were conducted using a stress-controlled rheometer (Physica MCR 301, Anton Paar, Austria) with a serrated parallel-plate geometry of 50 mm diameter and 1 mm gap. The linear viscoelastic region (LVR) was determined by strain amplitude sweep tests at a fixed angular frequency of 10 rad s^{-1}. The temperature sweep tests were performed at a constant angular frequency of 10 rad s^{-1} and a strain amplitude of 0.1%. A programmed heating-cooling process was used, i.e. heating from 20 to 100 ^{o}C, temperature hold at 100 ^{o}C for 10 min, and cooling from 100 to 20 ^{o}C with heating and cooling rate of 5 ^{o}C min^{-1}. Prevention of evaporation and temperature gradient were taken into account by using low-viscosity mineral oil and a peltier-controlled hood. Subsequently, frequency sweep tests were carried out from 0.5 to 50 rad

s^{-1} at constant strain amplitude of 0.1%. Frequency sweep data were correlated by means of the Power Law model using the following equations:

$$G' = a'\omega^{b'} \quad (1)$$

$$G" = a"\omega^{b"} \quad (2)$$

where ω, G', G", and are angular frequency, storage, and loss modulus respectively, and *a'*, *a"*, *b'*, and *b"* intercepts and slope of corresponding fitting parameters. Each test was run in duplicate.

3. Results and discussion

3.1. Assignment of OBPF chemical constituent in infrared spectra

Infrared spectra of OBPF are illustrated in Figure 1 showing chemical-bond vibrations of mixture system. Protein as the primary constituent can be traced by the presence of amide A, I, and II absorption bands. Amide A vibrations occurred at higher wavenumber and is contributed by N-H groups stretching vibrations. Amide I and II are predominantly induced by C=O and C-N stretching vibrations, and appear as two consecutive absorption signals between 1700 and 1500 cm^{-1} (Barth, 2007). The Amide A, I, and II absorption bands of OBPF appear at wavenumbers 3271, 1630, and 1517 cm^{-1} respectively. Evaluation of amide I region can provide useful information on protein secondary structure conformation which will be discussed in the later section.

Infrared spectral changes as affected by lipids and starch eliminations are presented in Table 1. Removal of neutral lipids by non-polar solvent drastically decreased the absorption signal at ~2924, ~2854, and ~1744 cm^{-1}. However, the use of polar solvent diminished the second peaks and left small signal of the third peak. This might indicate the asymmetric stretching vibrations of C-H at ~2924 cm^{-1} is not solely contributed by of lipid alone, but also from other major chemical constituents. The peak at ~2854 cm^{-1}

could be uniquely assigned to -CH_2- symmetric stretching of fatty acid chains. The peak ~1744 cm^{-1} corresponds to carbonyl (C=O) stretching vibration identifying the ester functional group of lipid (Cerqueira et al., 2012). Oats contain higher amounts of polar lipids compared to other cereals, such as glycolipids and monoacyl lipids (Doehlert et al., 2010).

Saccharide region of infrared spectra ranges from 1200 to 900 cm^{-1}. Three intense absorption bands at 1150, 1078, and 1022 cm^{-1} confirming typical vibration characteristics of C-O, C-C, O-H bonds and asymmetric stretching of C-O-C glycosidic bonds within the starch (Liu et al., 2011; Roa et al., 2014b). The strongest absorption band at 1022 cm^{-1} indicated predominant disordered conformational structure of OBPF starch that have gone through thermal treatment during production. This peak contains shoulder at the lower wavenumber that possibly indicate small amount of crystalline conformation. Alkaline exposure treatment dramatically decreased absorbance intensity of the three above mentioned peaks, indicating irreversible solubilisation of starch. This confirms the correct assignment for starch within infrared spectra and can be used to evaluate structural conformations in the later section.

3.2. Thermal properties of OBPF dispersions

The DSC thermograms and the corresponding thermal transition peak temperature and enthalpy changes of OBPF dispersions are presented in Figure 2 and Table 2 respectively. Upon the first heating, a broad endothermic peak appeared at c.a. 90 ^oC and consequently shifted to a higher temperature when reheated. Whereas upon cooling, a sharp exothermic peak was observed at c.a. 74 ^oC in either cycles. The ΔH values was 1.7 J g^{-1} on the first heating and subsequently decrease over the following cycles. The use of polar solvent greatly reduced ΔH values due to elimination of higher amounts of lipids as confirmed by

199 FTIR study. However, calorimetry scanning of extracted lipids did not show any thermal
200 transition events (data not shown). Starch solubilisation by alkaline exposure further
201 decreased the ΔH values. It shows that the ΔH values are more dependent to the starch
202 and lipids rather than the protein.

203 The reversible thermal events at very high temperature upon heating, i.e. 90 ^{o}C, can
204 be associated to the characteristics of starch-lipid complexes in the presence of protein
205 contained in thermally treated foods as found in previous studies (De Pilli et al., 2015;
206 Moisio et al., 2015; Wang et al., 2017). When the heated starch is cooled back in the
207 presence of lipid, the amylose recrystallize and form complexes with lipids by the
208 inclusion of fatty acid chain into helical cavity (Tufvesson et al., 2003). The amount of
209 amylose-lipid complexes is the major factor determining the ΔH value as proposed by
210 Kawai et al. (2012). Interestingly, melting temperature of starch-lipid complexes slightly
211 increased upon second heating hence indicating a more thermally-stable structure as a
212 result of complexes reformation in more ordered structure.

213

214 3.3.Ball milling effects on structural conformation of OBPF chemical constituents

215 Ball milling affected structural conformation changes on both protein and starch in
216 solid-state as illustrated in Figure 3 and Table 3. Prior to ball milling, secondary structure
217 of protein prominently presented as β-sheets structure and some minor helical structures.
218 This result demonstrated a higher composition in β-sheets compared to previous study on
219 oat protein isolate secondary structure at low moisture (Liu et al., 2009). The explanation
220 for this condition is the protein contained in OBPF has been thermally treated during the
221 production, hence most likely in denatured and aggregated form. The β-sheet structures
222 have been associated with hydrophobic and aggregated protein (Maltais et al., 2008;
223 Nikolaus Wellner et al., 2004; Tang and Ma, 2009). However, other study on oat protein

conformation in aqueous dispersion showed lower relative amount of β-sheets as the major structure (Jing et al., 2016). Secondary structure of protein in dispersion is a result from peptide-solvent interactions in aqueous environment, whereas at low moisture the peptide-peptide interactions are predominant factor due to dense packing in a solid environment.

Ball milling gradually increased relative amount of helical conformations in expense of β-sheet structures. Longer ball milling time, regardless the applied speed, demonstrated greater effect on protein conformational changes due to simultaneous mechanical impact. Similar result of increasing α -helix and decreasing β-sheet structure after ball milling soy protein isolate has been reported (Liu et al., 2017). Ball milling involves high pressure, shear force, and air contact that might cause rearrangement of aggregated protein secondary structure as suggested by Sun et al. (2015). Among the protein fractions and sub-units, low molecular weight proteins are the most susceptible to disruptions caused by ball milling (Thanatuksorn et al., 2009).

Evaluation of ball milling effects on starch conformation are presented in Table 3. A higher ratio of peak ~997 to ~1022 indicated small degree of ordered structure within starch conformation. The presence of amylose-lipid complexes has been reported to consists of some starch crystalline order (Kawai et al., 2012). In this study, longer ball milling time greatly reduced ordered structure of starch conformation. This ball milling effects on starch has been extensively studied in previous reports known by disruption effects on helical structures (Liu et al., 2011; Roa et al., 2015).

3.4. Ball milling effects on thermal properties of OBPF dispersions

Thermal properties of OBPF prior to and after ball milling are presented in Table 4. Ball milling did not greatly affect the transition peak temperature, whereas the enthalpy values gradually decreased as the milling time increased, regardless the applied speed.

Decreasing enthalpy values can be interpreted as the decrease on amounts of amylose-lipid complexes. This is confirmed by further loss of crystallinity provided by FTIR spectroscopy study. Simultaneous mechanical impact during ball milling disrupted the helical structure of amylose, hence disintegrated the amylose-lipid complexes. Ball milled samples did not differ in transition temperature peak upon the second heating showing thermal behaviour remain unchanged.

3.5. Ball milling effects on particle size distribution

Particle size distributions of OBPF prior to and after ball milling are presented in Figure 4 and Table 5. Prior to ball milling, wide range of particle size distributions were observed. The D_{10}, D_{50}, and D_{90} values represent 10, 50, and 90% particle size distributions within the dispersed sample, whereas the $D_{(4,3)}$ show average particle sizes. Ball milling at high speed reduced the particle size distributions to about quarter of initial values, e.g. from 116.45 ± 21.85 to 27.67 ± 0.93 μm. However, low speed ball milling could reduce to only about half of initial even after 360 min milling duration. This might be explained that rotational speed is a major factor to cause particle breakage during ball milling as suggested by Yin et al. (2015).

3.6. Ball milling effects on viscoelastic properties of OBPF dispersions

Figure 5 illustrated the viscoelastic properties of OBPF dispersions affected by ball milling and temperature changes. Ball milled samples at higher speed exhibited the lowest moduli at the same applied shear. Since the dispersions contain same weight fraction of samples, the volume packing fraction of HSST and LTST dispersions were lower, and hence decreased the storage moduli.

Temperature effects on moduli were observed in both heating and cooling cycles. Moduli decreases occurred below 40 ^{o}C seems to be the effects of increasing particle mobility since there were no thermal events recorded by scanning calorimetry within this temperature range. On the other hand, further decrease on moduli when temperature approached 90 ^{o}C indicate the melting of starch-lipid complexes contained in dispersions. Noticeable differences in melting behaviour of ball milled samples were observed using the tangent of phase angle (tan δ). Dispersions containing ball milled samples showed lower tan δ when reach the melting temperature that might due to the lower enthalpy changes.

The moduli of dispersions increased steadily upon cooling back to room temperature due to the recrystallisation of melted particles. Moreover, cooled dispersions reached higher moduli compared to initial values prior to heating. This might indicate the connectivity between particles were built during cooling which most likely contributed by starch.

Figure 6 illustrated the frequency-dependency of OBPF concentrated dispersions. The moduli increased with increase of angular frequency. Effects of ball milling were observed in the fitting parameters of frequency sweep data, presented in Table 6. Decreases in intercepts are consistent with the decreases of G' and G" due to particle volume packing effects. Ball milling also increased the slopes of moduli-frequency curves which revealed a weaker gel-like structure. As the particle volume packing decreases, solvent-particles interactions increase and inhibit the particle-particle interactions in building the structure. This is agreed with previous study on other flour dispersions (Ahmed et al., 2014). Both G' and G" of all samples were satisfactory fitted to Power Law's model, shown by the R^2 values close to 1.

4. Conclusions

Major constituent of OBPF were observed in the form of aggregated proteins and starch-lipid complexes. Ball milling altered the structural conformations of protein and starch, and reduced the enthalpy changes of starch-lipid complexes melting properties. Higher speed ball milling reduced particle size distributions to about quarter of initial values, e.g. from 116.45 ± 21.85 to 27.67 ± 0.93 μm, led to lower particle volume packing, and hence decreased the mechanical moduli of dispersions. Subsequent heating-cooling processes of OBPF dispersions allowed the starch to build a stronger networked structure. Therefore, the starch contained in OBPF plays as important constituent in influencing the structure of dispersion.

Acknowledgments

The first author would like express gratitude to the Ministry of Research, Technology, and Higher Education of the Republic of Indonesia for the financial support.

References

Abbaszadeh, A., MacNaughtan, W., Foster, T.J., 2014. The effect of ball milling and rehydration on powdered mixtures of hydrocolloids. Carbohydr. Polym. 102, 978–985. doi:10.1016/j.carbpol.2013.10.020

Ahmed, J., Al-Foudari, M., Al-Salman, F., Almusallam, A.S., 2014. Effect of particle size and temperature on rheological, thermal, and structural properties of pumpkin flour dispersion. J. Food Eng. 124, 43–53. doi:10.1016/j.jfoodeng.2013.09.030

Barth, A., 2007. Infrared spectroscopy of proteins. Biochim. Biophys. Acta - Bioenerg. 1767, 1073–1101. doi:10.1016/j.bbabio.2007.06.004

Cerqueira, M.A., Souza, B.W.S., Teixeira, J.A., Vicente, A.A., 2012. Effect of glycerol and

corn oil on physicochemical properties of polysaccharide films – A comparative study. Food Hydrocoll. 27, 175–184. doi:10.1016/j.foodhyd.2011.07.007

De Pilli, T., Legrand, J., Derossi, A., Severini, C., 2015. Effect of proteins on the formation of starch-lipid complexes during extrusion cooking of wheat flour with the addition of oleic acid. Int. J. Food Sci. Technol. 50, 515–521. doi:10.1111/ijfs.12698

De Souza, D., Sbardelotto, A.F., Ziegler, D.R., Marczak, L.D.F., Tessaro, I.C., 2016. Characterization of rice starch and protein obtained by a fast alkaline extraction method. Food Chem. 191, 36–44. doi:10.1016/j.foodchem.2015.03.032

Deutz, N.E.P., Bauer, J.M., Barazzoni, R., Biolo, G., Boirie, Y., Bosy-Westphal, A., Cederholm, T., Cruz-Jentoft, A., Krznariç, Z., Nair, K.S., Singer, P., Teta, D., Tipton, K., Calder, P.C., 2014. Protein intake and exercise for optimal muscle function with aging: Recommendations from the ESPEN Expert Group. Clin. Nutr. 33, 929–936. doi:10.1016/j.clnu.2014.04.007

Dhital, S., Shrestha, A.K., Flanagan, B.M., Hasjim, J., Gidley, M.J., 2011. Cryo-milling of starch granules leads to differential effects on molecular size and conformation. Carbohydr. Polym. 84, 1133–1140. doi:10.1016/j.carbpol.2011.01.002

Doehlert, D.C., Moreau, R.A., Welti, R., Roth, M.R., McMullen, M.S., 2010. Polar lipids from oat kernels. Cereal Chem. 87, 467–474. doi:10.1094/CCHEM-04-10-0060

Jing, X., Yang, C., Zhang, L., 2016. Characterization and Analysis of Protein Structures in Oat Bran. J. Food Sci. 81, C2337–C2343. doi:10.1111/1750-3841.13445

Jodayree, S., Smith, J.C., Tsopmo, A., 2012. Use of carbohydrase to enhance protein extraction efficiency and antioxidative properties of oat bran protein hydrolysates. Food Res. Int. 46, 69–75. doi:10.1016/j.foodres.2011.12.004

Kawai, K., Takato, S., Sasaki, T., Kajiwara, K., 2012. Complex formation, thermal properties, and in-vitro digestibility of gelatinized potato starch-fatty acid mixtures.

348 Food Hydrocoll. 27, 228–234. doi:10.1016/j.foodhyd.2011.07.003
349 Konak, Ü.İ., Ercili-Cura, D., Sibakov, J., Sontag-Strohm, T., Certel, M., Loponen, J., 2014.
350 CO2-defatted oats: Solubility, emulsification and foaming properties. J. Cereal Sci. 60,
351 37–41. doi:10.1016/j.jcs.2014.01.013
352 Liu, B., Wang, H., Hu, T., Zhang, P., Zhang, Z., Pan, S., Hu, H., 2017. Ball-milling changed
353 the physicochemical properties of SPI and its cold-set gels. J. Food Eng. 195, 158–165.
354 doi:10.1016/j.jfoodeng.2016.10.006
355 Liu, G., Li, J., Shi, K., Wang, S., Chen, J., Liu, Y., Huang, Q., 2009. Composition, secondary
356 structure, and self-assembly of oat protein isolate. J. Agric. Food Chem. 57, 4552–4558.
357 doi:10.1021/jf900135e
358 Liu, T.Y., Ma, Y., Yu, S.F., Shi, J., Xue, S., 2011. The effect of ball milling treatment on
359 structure and porosity of maize starch granule. Innov. Food Sci. Emerg. Technol. 12,
360 586–593. doi:10.1016/j.ifset.2011.06.009
361 Maltais, A., Remondetto, G.E., Subirade, M., 2008. Mechanisms involved in the formation
362 and structure of soya protein cold-set gels: A molecular and supramolecular
363 investigation. Food Hydrocoll. 22, 550–559. doi:10.1016/j.foodhyd.2007.01.026
364 Moisio, T., Forssell, P., Partanen, R., Damerau, A., Hill, S.E., 2015. Reorganisation of starch,
365 proteins and lipids in extrusion of oats. J. Cereal Sci. 64, 48–55.
366 doi:10.1016/j.jcs.2015.04.001
367 Nikolaus Wellner, *,†, E. N. Clare Mills, †, Geoff Brownsey, †, Reginald H. Wilson, †, Neil
368 Brown, ‡, Jacqueline Freeman, ‡, Nigel G. Halford, ‡, Peter R. Shewry, ‡ and, Belton§,
369 P.S., 2004. Changes in Protein Secondary Structure during Gluten Deformation Studied
370 by Dynamic Fourier Transform Infrared Spectroscopy. doi:10.1021/BM049584D
371 Pandey, R., Shrivastava, S.L., 2017. Comparative evaluation of rice bran oil obtained with
372 two-step microwave assisted extraction and conventional solvent extraction. J. Food

373 Eng. 218, 106–114. doi:10.1016/j.jfoodeng.2017.09.009
374 Puncha-Arnon, S., Uttapap, D., 2013. Rice starch vs. rice flour: Differences in their
375 properties when modified by heat-moisture treatment. Carbohydr. Polym. 91, 85–91.
376 doi:10.1016/j.carbpol.2012.08.006
377 Roa, D.F., Baeza, R.I., Tolaba, M.P., 2015. Effect of ball milling energy on rheological and
378 thermal properties of amaranth flour. J. Food Sci. Technol. 52, 8389–8394.
379 doi:10.1007/s13197-015-1976-z
380 Roa, D.F., Santagapita, P.R., Buera, M.P., Tolaba, M.P., 2014a. Ball Milling of Amaranth
381 Starch-Enriched Fraction. Changes on Particle Size, Starch Crystallinity, and
382 Functionality as a Function of Milling Energy. Food Bioprocess Technol. 7, 2723–2731.
383 doi:10.1007/s11947-014-1283-0
384 Roa, D.F., Santagapita, P.R., Buera, M.P., Tolaba, M.P., 2014b. Amaranth Milling Strategies
385 and Fraction Characterization by FT-IR. Food Bioprocess Technol. 7, 711–718.
386 doi:10.1007/s11947-013-1050-7
387 Saleh, M.I., 2017. Protein-starch matrix microstructure during rice flour pastes formation. J.
388 Cereal Sci. 74, 183–186. doi:10.1016/j.jcs.2017.02.005
389 Sozer, N., Nordlund, E., Ercili-Cura, D., Poutanen, K., 2017. Cereal Side-Streams as
390 Alternative Protein Sources. Cereal Foods World 62, 132–137. doi:10.1094/CFW-62-4-
391 0132
392 Sun, C., Liu, R., Wu, T., Liang, B., Shi, C., Zhang, M., 2015. Effect of superfine grinding on
393 the structural and physicochemical properties of whey protein and applications for
394 microparticulated proteins. Food Sci. Biotechnol. 24, 1637–1643. doi:10.1007/s10068-
395 015-0212-y
396 Tang, C.-H., Ma, C.-Y., 2009. Effect of high pressure treatment on aggregation and structural
397 properties of soy protein isolate. LWT - Food Sci. Technol. 42, 606–611.

doi:10.1016/j.lwt.2008.07.012

Thanatuksorn, P., Kawai, K., Kajiwara, K., Suzuki, T., 2009. Effects of ball-milling on the glass transition of wheat flour constituents. J. Sci. Food Agric. 89, 430–435. doi:10.1002/jsfa.3463

Tufvesson, F., Wahlgren, M., Eliasson, A.C., 2003. Formation of amylose-lipid complexes and effects of temperature treatment - Part 1. Monoglycerides. Starch/Stärke 55, 61–71. doi:10.1002/star.200390018

Wang, S.S., Zheng, M., Yu, J., Wang, S.S., Copeland, L., 2017. Insights into the Formation and Structures of Starch-Protein-Lipid Complexes. J. Agric. Food Chem. 65, 1960–1966. doi:10.1021/acs.jafc.6b05772

Westerterp-Plantenga, M.S., Lemmens, S.G., Westerterp, K.R., 2017. Dietary protein – its role in satiety, energetics, weight loss and health. doi:10.1017/S0007114512002589

Yin, T., Park, J.W., Xiong, S., 2015. Physicochemical properties of nano fish bone prepared by wet media milling. LWT - Food Sci. Technol. 64, 367–373. doi:10.1016/j.lwt.2015.06.007

Figure 1

Click here to download high resolution image

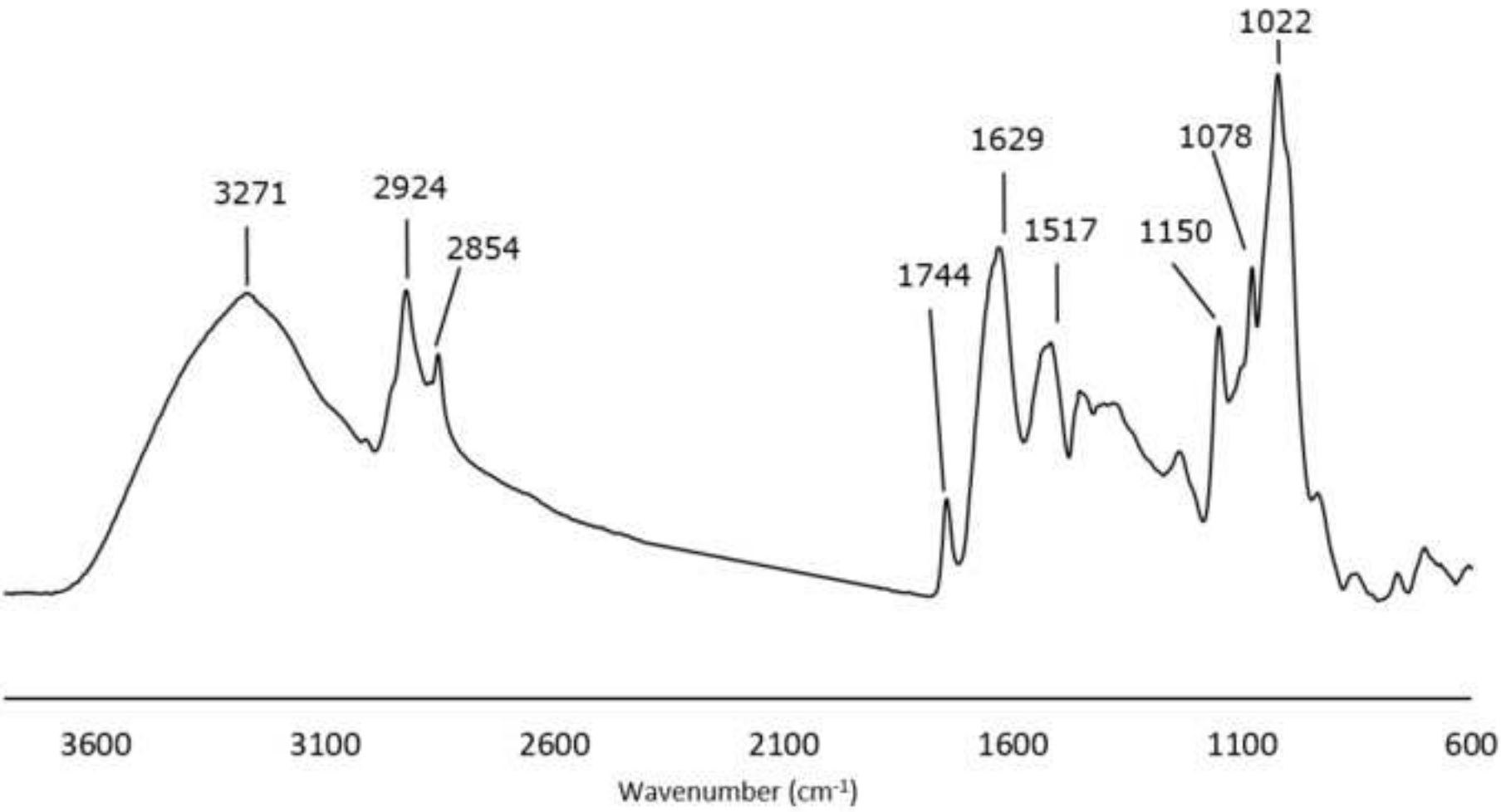

Figure 2

Click here to download high resolution image

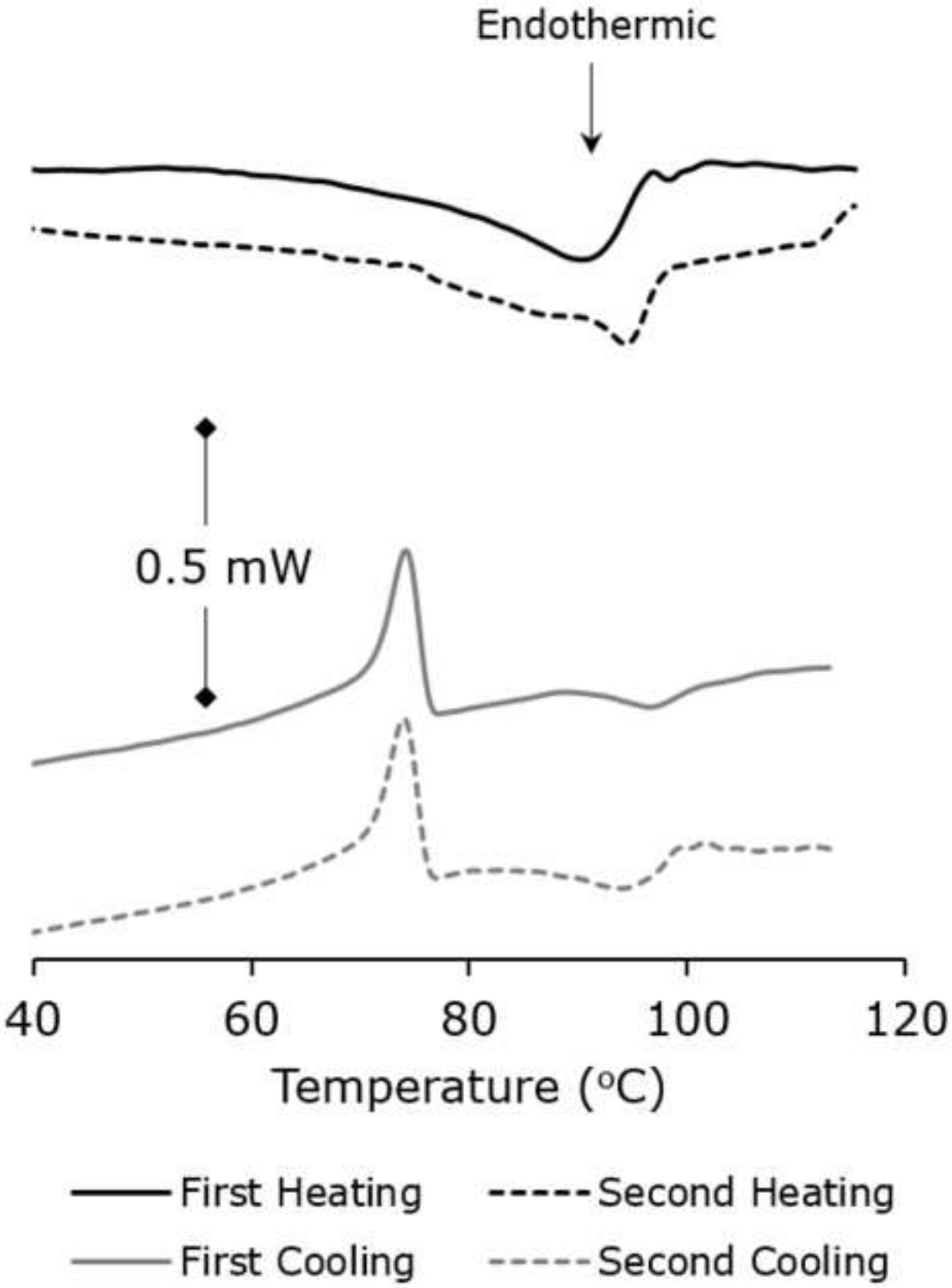

Figure 3

Click here to download high resolution image

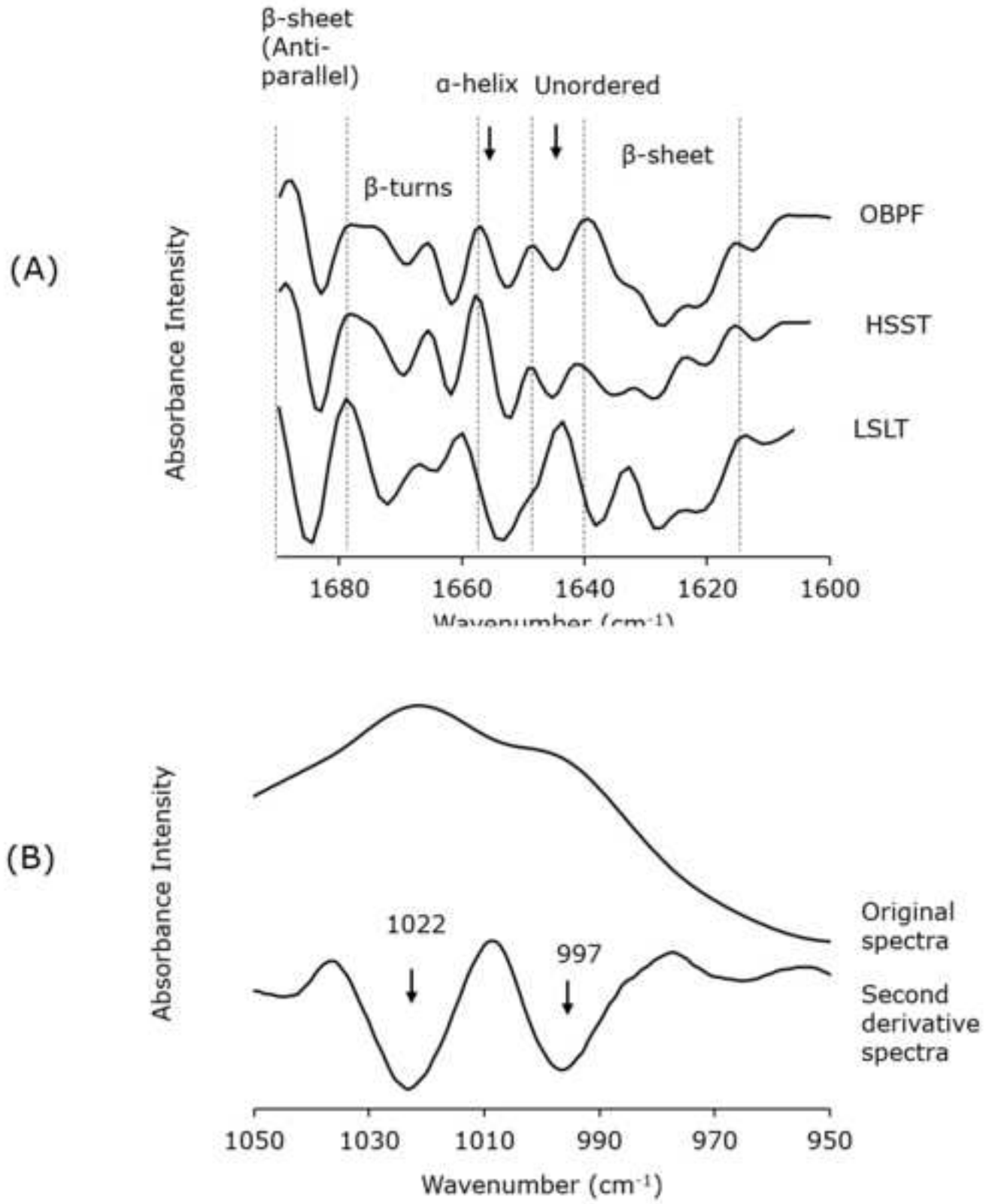

Figure 4

Click here to download high resolution image

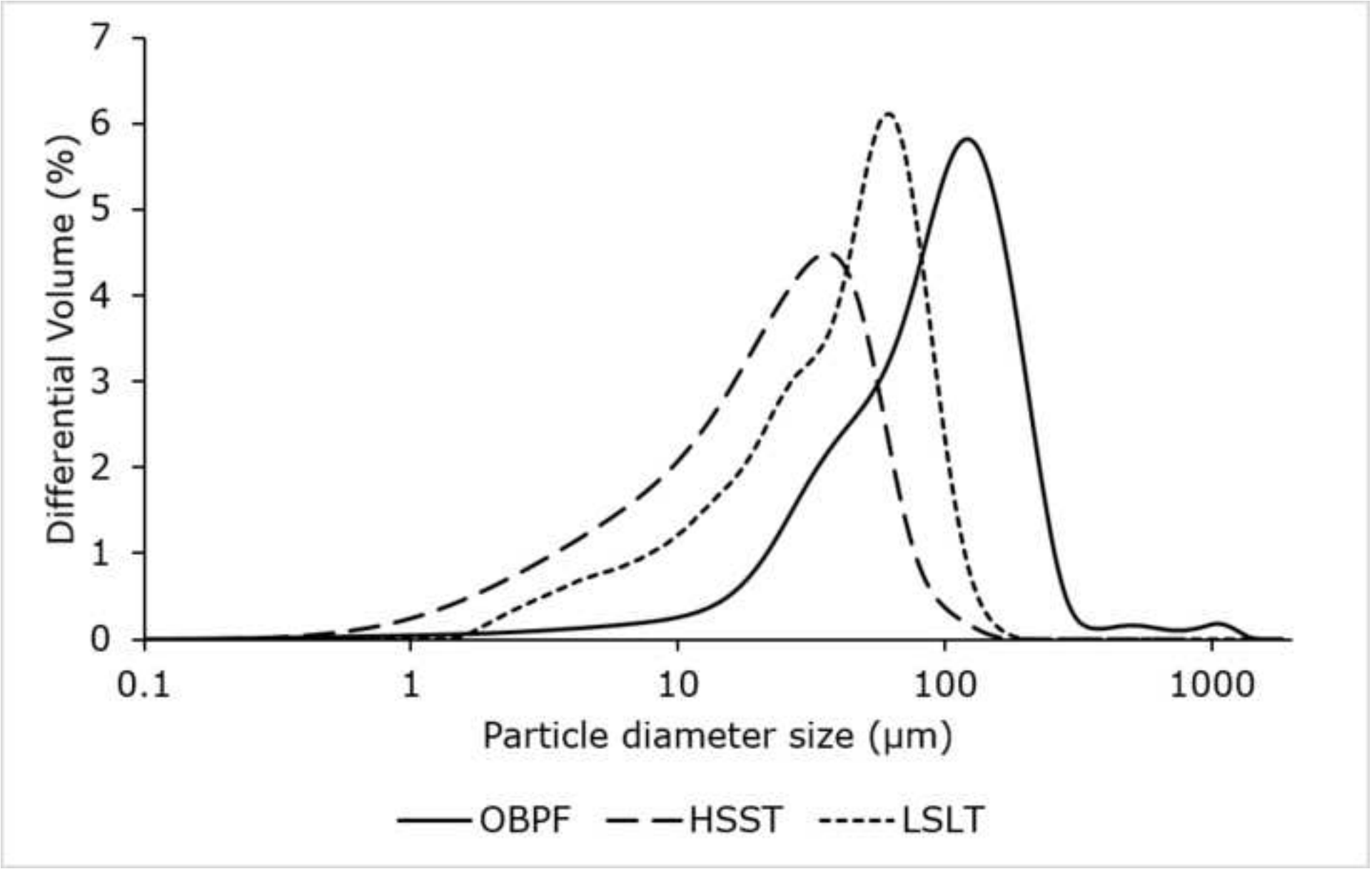

Figure 5

Click here to download high resolution image

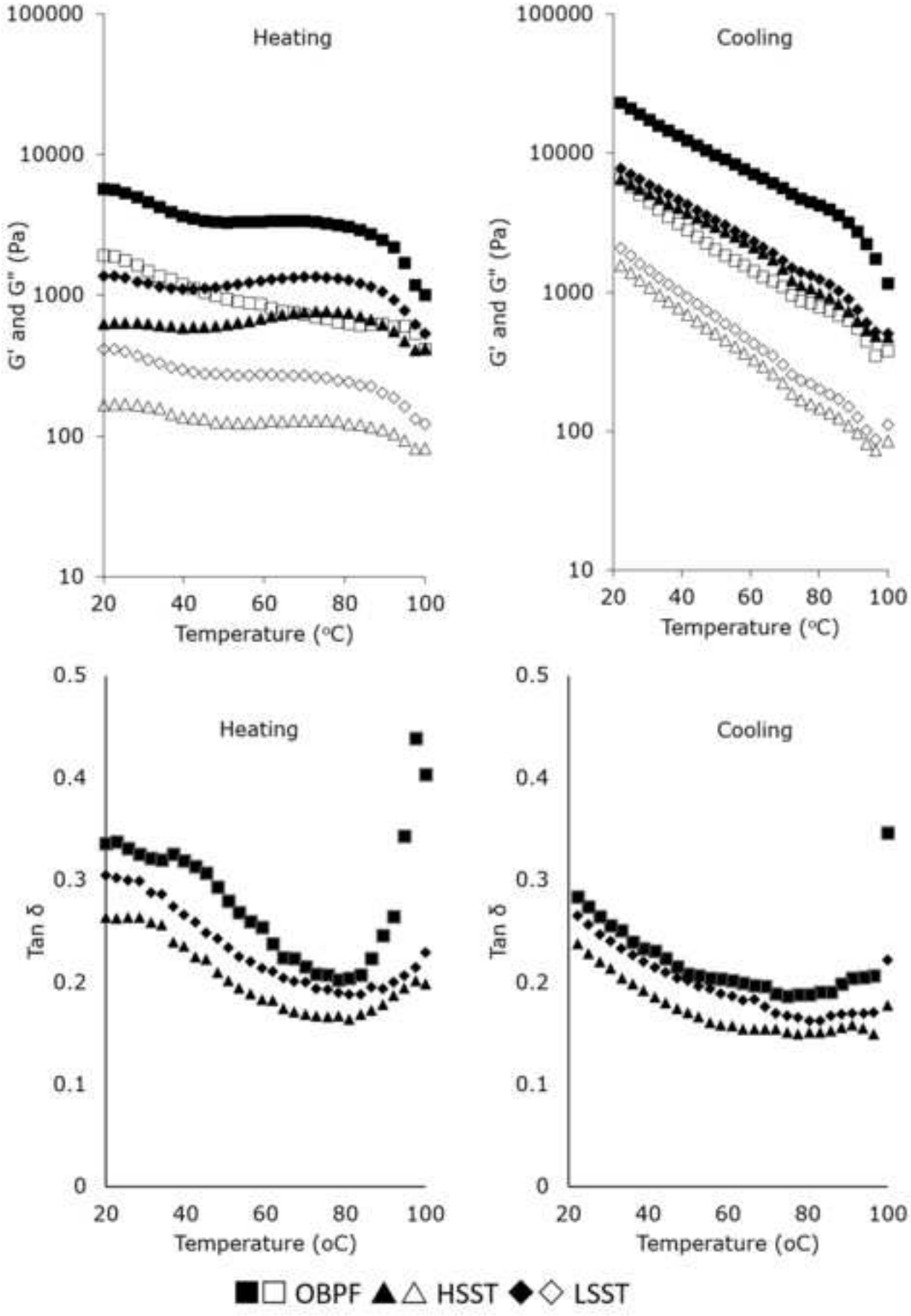

Figure 6

Click here to download high resolution image

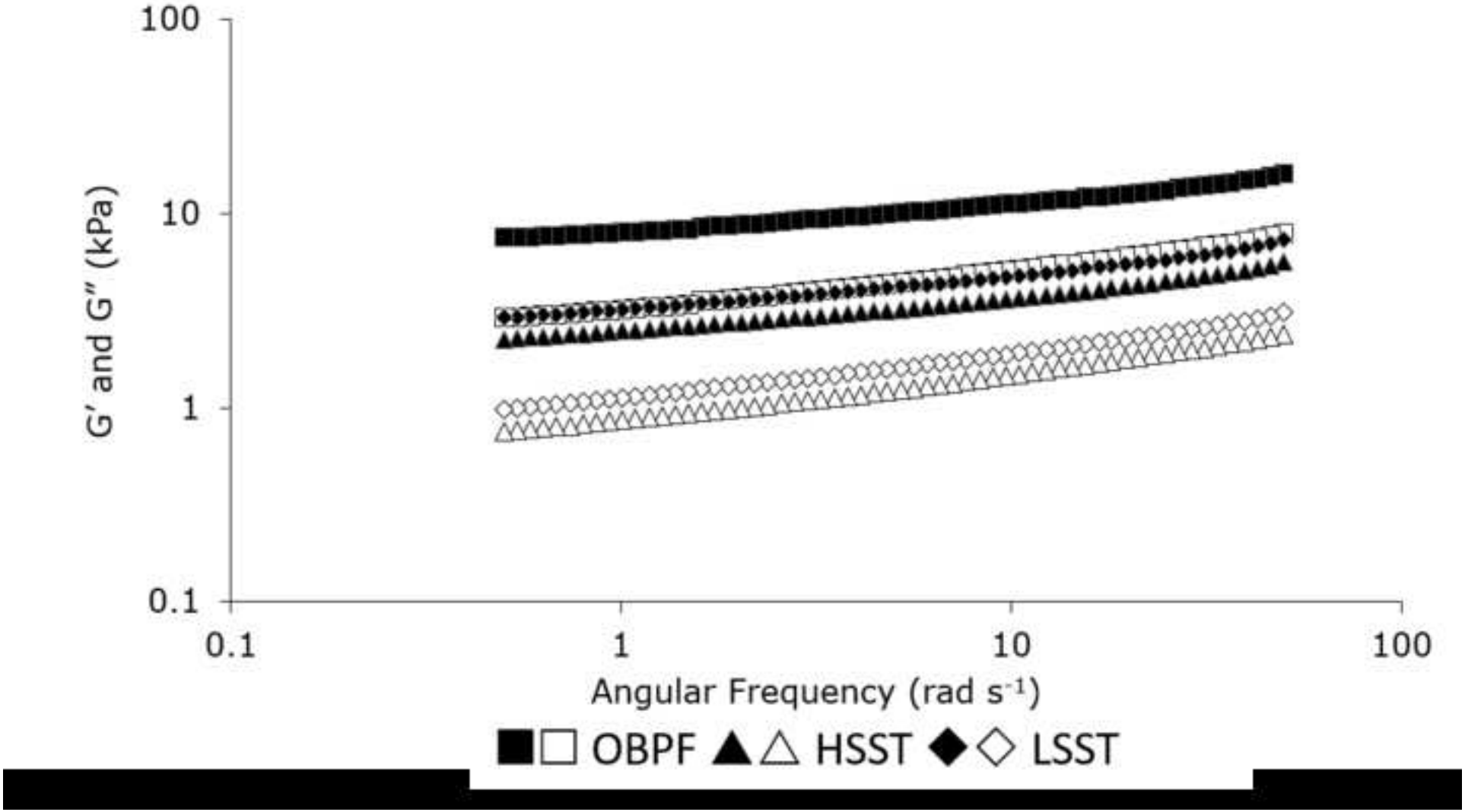

Figure captions

Figure 1 Typical infrared spectra of oat bran protein flour

Figure 2 DSC thermogram of OBPF dispersions upon heating-cooling cycles

Figure 3 (A) Second derivative spectra at amide I region of OBPF prior to and after ball milling; (B) original and second derivative spectra of OBPF at saccharide region. For abbreviations see Table 3.

Figure 4 Volume-weighted particle size distributions of OBPC prior to and after ball milling. For abbreviations see Table 3.

Figure 5 Storage (filled) and loss (open) moduli (top), and tangent of phase angle (bottom) of OBPC concentrated dispersions prior to and after ball milling over changing temperatures. For abbreviations see Table 3.

Figure 6 Storage (filled) and loss (open) moduli of OBPC concentrated dispersions prior to and after ball milling over changing angular frequencies. For abbreviations see Table 3.

Table 1. Infrared spectral changes on selected bands of OBPF and its derived fractions

Sample	Peak height ratio relative to peak at ~1630 cm^{-1}					
	~2924 cm^{-1}	~2854 cm^{-1}	~1744 cm^{-1}	~1150 cm^{-1}	~1078 cm^{-1}	~1022 cm^{-1}
OBPF	0.55 ± 0.04	0.11 ± 0.02	0.32 ± 0.02	0.67 ± 0.05	0.49 ± 0.06	0.94 ± 0.14
NPDO	0.31 ± 0.02	0.02 ± 0.00	0.16 ± 0.08	0.69 ± 0.06	0.53 ± 0.06	0.92 ± 0.03
PDO	0.29 ± 0.01	N/A	0.08 ± 0.01	0.79 ± 0.08	0.54 ± 0.08	1.02 ± 0.15
APDO	0.21 ± 0.02	N/A	0.05 ± 0.01	0.48 ± 0.06	0.37 ± 0.04	0.61 ± 0.12

Abbreviations: OBPF (Oat bran protein flour), NPDO (Non polar solvent defatted OBPF), PDO (Polar solvent defatted OBPF), APDO (Alkaline exposed PDO).

Table 2. Thermal transition peak temperatures (T_p) and enthalpy changes (ΔH) of OBPF dispersions and its derived fractions

Sample	First heating		First cooling		Second heating		Second cooling	
	T_p (^oC)	ΔH (J g^{-1} solid)	T_p (^oC)	ΔH (J g^{-1} solid)	T_p (^oC)	ΔH (J g^{-1} solid)	T_p (^oC)	ΔH (J g^{-1} solid)
OBPF	90.63 ± 0.32	1.70 ± 0.21	74.14 ± 0.04	-1.02 ± 0.04	94.42 ± 0.10	1.01 ± 0.02	73.97 ± 0.04	-0.94 ± 0.02
NPDO	91.12 ± 0.74	0.94 ± 0.18	74.49 ± 0.05	-0.84 ± 0.02	94.98 ± 0.08	0.72 ± 0.13	74.34 ± 0.03	-0.72 ± 0.07
PDO	90.41 ± 0.59	0.76 ± 0.02	73.80 ± 0.25	-0.64 ± 0.04	94.07 ± 0.16	0.61 ± 0.04	73.73 ± 0.25	-0.53 ± 0.08
APDO	92.07 ± 0.51	0.48 ± 0.01	72.28 ± 0.41	-0.32 ± 0.02	92.76 ± 0.16	0.26 ± 0.02	71.88 ± 0.61	-0.26 ± 0.05

For abbreviations see Table 1.

Table 3. Ball milling effects on protein and starch structural conformation

Sample	Relative area of protein secondary structure bands (%)		Starch
	Total β-sheets and β-turns (%)	Total α-helix and random coil (%)	~997/~1022 cm^{-1} ratio
OBPF	88.03 ± 2.69	11.97 ± 2.69	0.63 ± 0.02
HSST10	82.33 ± 2.68	17.67 ± 2.68	0.57 ± 0.06
HSST20	82.53 ± 1.02	17.47 ± 1.02	0.56 ± 0.05
HSST30	79.85 ± 0.61	20.15 ± 0.61	0.50 ± 0.02
LSLT120	80.96 ± 4.39	19.04 ± 4.39	0.56 ± 0.04
LSLT240	81.88 ± 1.38	18.12 ± 1.38	0.49 ± 0.04
LSLT360	80.33 ± 6.95	19.67 ± 6.95	0.38 ± 0.04

Abbreviations: OBPF (Oat bran protein flour), HSST10, 20, and 30 (Ball milled OBPF at high speed, i.e. 800 rpm for short time, i.e. 10, 20, or 30 min), LSLT120, 240, and 360 (Ball milled OBPF at low speed, i.e. 200 rpm for long time, i.e. 120, 240, or 360 min)

Table 4. Thermal transition peak temperatures and enthalpy changes of OBPF dispersions affected by ball milling

Sample	First heating		First cooling		Second heating		Second cooling	
	T_p (^oC)	ΔH (J g^{-1} solid)	T_p (^oC)	ΔH (J g^{-1} solid)	T_p (^oC)	ΔH (J g^{-1} solid)	T_p (^oC)	ΔH (J g^{-1} solid)
OBPF	90.63 ± 0.32	1.70 ± 0.21	74.14 ± 0.04	-1.02 ± 0.04	94.42 ± 0.10	1.01 ± 0.02	73.97 ± 0.04	-0.94 ± 0.02
HSST30	90.50 ± 0.26	1.19 ± 0.14	73.72 ± 0.09	-0.78 ± 0.07	94.10 ± 0.01	0.65 ± 0.12	73.63 ± 0.10	-0.51 ± 0.01
LSLT360	91.20 ± 0.34	0.85 ± 0.07	74.04 ± 0.09	-0.77 ± 0.07	94.52 ± 0.07	0.66 ± 0.10	73.96 ± 0.07	-0.60 ± 0.04

For abbreviations see Table 3.

Table 5. Particle size distributions OBPF prior to and after ball milling

Sample	$D_{(4,3)}$ (µm)	D_{10} (µm)	D_{50} (µm)	D_{90} (µm)
OBPF	116.45 ± 21.85	27.33 ± 0.80	98.11 ± 5.79	203.50 ± 21.92
HSST	27.67 ± 0.93	4.09 ± 0.10	23.22 ± 0.47	56.67 ± 1.66
LSLT	49.33 ± 0.23	10.01 ± 0.86	46.88 ± 0.36	91.55 ± 0.05

For abbreviations see Table 3.

Table 6. Parameters of moduli-frequency fitting based on the Power Law model

Sample	G’			G”		
	a' (kPa)	b'	R^2	a' (kPa)	b'	R^2
OBPF	7.94 ± 0.93	0.16 ± 0.00	0.986 ± 0.008	3.18 ± 0.17	0.21 ± 0.01	0.992 ± 0.004
HSST	2.44 ± 0.11	0.19 ± 0.05	0.985 ± 0.005	0.85 ± 0.35	0.24 ± 0.02	0.994 ± 0.002
LSLT	3.15 ± 0.67	0.19 ± 0.04	0.988 ± 0.002	1.11 ± 0.02	0.24 ± 0.02	0.994 ± 0.003

For abbreviations see Table 3.